Journal of Power Sources 260 (2014) 264–267

Contents lists available at ScienceDirect

Journal of Power Sources

journal homepage: www.elsevier.com/locate/jpowsour

Short communication

High performance Li_2S—P_2S_5 solid electrolyte induced by selenide

Zhanqiang Liu [a], Yufeng Tang [a], Yaoming Wang [a], Fuqiang Huang [a,b,*]

[a] CAS Key Laboratory of Materials for Energy Conversion, Shanghai Institute of Ceramics, Chinese Academy of Sciences, Shanghai 200050, PR China
[b] State Key Laboratory of Rare Earth Materials Chemistry and Applications, College of Chemistry and Molecular Engineering, Peking University, Beijing 100871, PR China

HIGHLIGHTS

- Nonhygroscopic and chemically stable selenide is introduced into Li_2S—P_2S_5.
- A high ionic conductivity 1.5 × 10^{-3} S cm^{-1} at room temperature is achieved.
- The obtained solid electrolyte has a wide electrochemical window over 6.5 V.
- Double substitution effect results in the high lithium ion conductivity.

ARTICLE INFO

Article history:
Received 21 October 2013
Received in revised form
24 January 2014
Accepted 12 March 2014
Available online 19 March 2014

Keywords:
Solid electrolyte
Selenide
Glass-ceramics
Double substitution effect

ABSTRACT

Nonhygroscopic selenide of $Ge_{0.35}Ga_{0.05}Se_{0.60}$ was introduced into the Li_2S—P_2S_5 system by partially substituting P_2S_5 to form a new lithium ion solid electrolyte. And the electrochemical property of the as-prepared solid electrolyte was systematically studied. The optimal sample achieved a wide electrochemical window over 6.5 V and fairly high Li-ion conductivity of 1.5 × 10^{-3} S cm^{-1} at ambient temperature. And it is also verified that the studied electrolyte was much stable when contacts with lithium metal at 100 °C for 4 h. This new finding may provide an electrolyte material for developing all-solid-state lithium batteries.

© 2014 Elsevier B.V. All rights reserved.

1. Introduction

Lithium solid electrolytes (LiSEs) have been attracting extensive attention in the research and application of lithium ion secondary batteries during recent decades. The intrinsic advantages include high thermal stability, absence of leakage or pollution, resistance to shock or vibration, and wide electrochemical window [1–4]. Many oxides and sulfides have been investigated as LiSEs, and some exhibit fairly good properties [4–9]. The glassy sulfide system of Li_2S—P_2S_5 exhibits high ion conductivity over 10^{-4} S cm^{-1} at room temperature and has become an important electrolyte system [9–12]. However, much higher ion conductivity is still in great demand for all-solid-state batteries, furthermore the hygroscopic feature of P_2S_5 brings much inconvenience for the practical application. The $Li_{10}GeP_2S_{12}$ (LGPS) superionic conductor (the ion conductivity: 10^{-2} S cm^{-1} [5]) faces the same hygroscopic problem.

Compared with oxides and sulfides, selenide-containing compounds possess several potential advantages as LiSEs: (1) the larger ion radius of Se^{2-} indicates bigger channels for Li^+ transfer, (2) the less electronegativity of Se implies a weaker attractive force between Li^+ and the frame structure, and (3) the higher polarizability of Se^{2-} will further facilitate the mobility of Li^+. However, the worries about the instability in contact with lithium and the predicated relatively narrow electrochemical window prevent researchers investigating the feasibility of using them as LiSEs. Only a few selenide-containing compounds were reported as LiSEs [13–15]. Although the lithium ion conductivities of the sulfides were increased after S^{2-} replaced by Se^{2-}, they were still in the same order of magnitude. So the replacement of S^{2-} by Se^{2-} has not been considered be a good solution to enhance the lithium ion conductivity.

Here, the nonhygroscopic and chemically stable $Ge_{0.35}Ga_{0.05}Se_{0.60}$ [16] was selected to introduce into the hygroscopic sulfides. We partially substituted P_2S_5 with $Ge_{0.35}Ga_{0.05}Se_{0.60}$ in Li_2S—P_2S_5 system to prepare a selenide-containing LiSE. As a control experiment,

* Corresponding author. CAS Key Laboratory of Materials for Energy Conversion, Shanghai Institute of Ceramics, Chinese Academy of Sciences, Shanghai 200050, PR China. Tel.: +86 21 5241 1620; fax: +86 21 5241 6360.
E-mail address: huangfq@mail.sic.ac.cn (F. Huang).

http://dx.doi.org/10.1016/j.jpowsour.2014.03.036
0378-7753/© 2014 Elsevier B.V. All rights reserved.

partial substitution of P_2S_5 with $Ge_{0.35}Ga_{0.05}S_{0.60}$ in Li_2S–P_2S_5 system was also conducted to elucidate the effect of selenium.

2. Experimental

Li_2S was prepared by the reaction of lithium and sulfur in liquid ammonia. P_2S_5 and $Ge_{0.35}Ga_{0.05}Q_{0.60}$ (Q = S, Se) were synthesized by sintering the stoichiometric elements in evacuated sealed silica tubes for 24 h at 650 °C and 950 °C, respectively. The raw materials were well mixed according to the stoichiometric of $0.5Li_2S$–xP_2S_5–$(1-x)Ge_{0.35}Ga_{0.05}Q_{0.60}$ (x = 0.1, 0.3, 0.5, 0.7, 0.9), and calcined at 750 °C for 10 h in evacuated silica tubes. Consequently, the tubes were quenched in cold water. The as-prepared sample with the highest ionic conductivity was selected and mechanically milled in a high-energy ball miller (SPEX CertiPrep 8000 Mixer/Mill) to further improve its ion conductivity property.

X-ray diffraction measurements were performed using a diffractometer (Rigaku D/Max-2550 V, 40 kV, 40 mA, Cu K_α, λ = 1.5406 Å) to identify the crystal phases.

For ionic conductivity measurement, each powder sample was cold-pressed into a $\phi 10 \times 1$ mm pellet and both sides of the pellet were attached with indium plates as current collectors. Then the measurement was conducted in a dry argon flow by complex impedance on an impedance analyzer (Chenhua 660C) in the frequency range of 0.1 Hz and 0.1 MHz over the temperature range from 30 °C to 150 °C.

DC polarization measurements were carried out to determine the electronic conductivity. Indium foils were used as blocking electrodes and lithium plates as unblocking electrodes. Time dependence of the electrical currents was measured under a constant voltage of 1 V for 1000 s.

In order to determine the chemical stability of the electrolyte in contact with lithium metal, DC polarization measurements on the heat-treated samples (100 °C × 4 h) were also carried out.

Cyclic voltammogram (CV) of the asymmetric Li/sample/Pt cell was also performed on Chenhua 660C to evaluate the electrochemical stability of the electrolytes. Li and Pt were used as the reference/counter and working electrodes, respectively. The scan rate was 1 mV s^{-1} and the scan range was from −0.4 to +6.5 V *vs.* Li^+/Li.

3. Results and discussion

Fig. 1 shows the composition dependence of ionic conductivities at 30 °C ($\sigma_{30°C}$) and the activation energies (E_a) of $0.5Li_2S$–xP_2S_5–$(1-x)Ge_{0.35}Ga_{0.05}Q_{0.60}$ (Q = S, Se). The replacing of P_2S_5 with either $Ge_{0.35}Ga_{0.05}S_{0.60}$ or $Ge_{0.35}Ga_{0.05}Se_{0.60}$ when $x \leq 0.5$ steadily increases the lithium ion conductivity, while further substitution ($x > 0.5$) gradually decreases the conductivity of the system. And the ionic conductivity of the sample introduced with $Ge_{0.35}Ga_{0.05}Se_{0.60}$ is about one order of magnitude higher than that introduced with the same amount of $Ge_{0.35}Ga_{0.05}S_{0.60}$. This directly demonstrates that Se^{2-} is more advantageous for lithium ion conducting than S^{2-}.

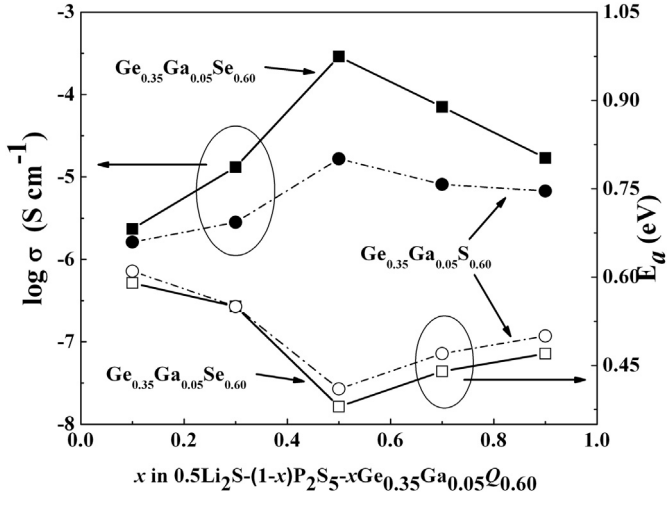

Fig. 1. Variation of $\sigma_{30°C}$ and E_a as the function of x in $0.5Li_2S$–xP_2S_5–$(1-x)Ge_{0.35}Ga_{0.05}Q_{0.60}$ (Q = S, Se).

The comparison of ionic conductivities difference between $Li_{10}GeP_2S_{12}$ [5] and $Li_{10}GeP_2Se_{12}$ [5,15], or between Li_4SnS_4 [17] and Li_4SnSe_4 [14] has indicated that the crystal structure of $Li_{10}GeP_2S_{12}$ or Li_4SnS_4 has an "ideal" diffusion channel for Li^+ transport. Consequently, the substitution of S by Se in $Li_{10}GeP_2S_{12}$ slightly enhanced the lithium ion conductivity from 1.3×10^{-2} S cm^{-1} to 2.4×10^{-2} S cm^{-1}. The lithium ion conductivity of amorphous Li_2S–P_2S_5 was also only increased from 2.4×10^{-4} S cm^{-1} to 6.0×10^{-4} S cm^{-1} with P_2S_5 slightly substituted by P_2Se_5 [13]. With increasing the content of P_2Se_5 higher than 8%, the conductivity decreased reversely. In our investigated system of $0.5Li_2S$–xP_2S_5–$(1-x)Ge_{0.35}Ga_{0.05}Se_{0.60}$, crystalline nanoparticles of $0.5Li_2S$–xP_2S_5 are covered by amorphous glass $Ge_{0.35}Ga_{0.05}Se_{0.60}$. At the interface between $0.5Li_2S$–xP_2S_5 and $Ge_{0.35}Ga_{0.05}Se_{0.60}$, double substitution effect exists, which means partial substitutions of Se at the S sites and Ge at the P sites can be formed during annealing. Thus the interface area is much suitable for lithium ion to transfer and the enhancement of lithium ion conductivity of the sample can be achieved.

The sample with the highest lithium ion conductivity, $0.5Li_2S$–$0.5P_2S_5$–$0.5Ge_{0.35}Ga_{0.05}Se_{0.60}$, was selected for further high-energy ball milling for 0, 4 and 12 h, respectively. The as-prepared samples were labeled as Sample 1, Sample 2 and Sample 3, respectively. The XRD patterns of the above three samples are shown in Fig. 2. Halo patterns can be observed, indicating the primary presence of amorphous phases. Sample 1 is one of the typical quenched sample without further milling treatment. The quenching process was only conducted by dropping the samples into cold water after taking out at the temperature of 750 °C. With this kind of process, the samples were not thoroughly quenched. Then the quenched samples should be in the form of glass-ceramic state.

Kanno and Murayama [8] have reported that the sulfide lithium superionic conductor (thio-LISICON) $Li_{4-x}Ge_{1-x}P_xS_4$ can be divided into three composition regions: Region I ($0 < x < 0.6$), II ($0.6 < x < 0.8$), and III ($0.8 < x < 1.0$), and the highest ionic conductivity was observed in Region II. The XRD pattern of Sample 1

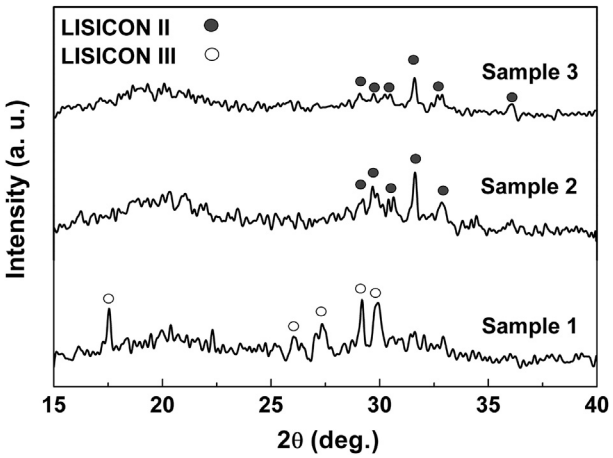

Fig. 2. XRD patterns of Sample 1, Sample 2 and Sample 3.

(without milling) is similar to that of the thio-LISICON phase in the region III (thio-LISICON III). While the patterns of Sample 2 and Sample 3 (ball-milled) are similar to that of the thio-LISICON phase in the region II (thio-LISICON II). It indicates that highly conductive thio-LISICON phase was formed, and a phase transition from thio-LISICON III analog to thio-LISICON II analog was induced by the high-energy ball-milling. It can be inferred from the results that the substitution of Ge at the P sites were still inefficient at the interface between $0.5Li_2S–xP_2S_5$ and $Ge_{0.35}Ga_{0.05}Se_{0.60}$ at conditions of 750 °C for 10 h. After further milling treatment, the substitution was increased with Ge diffusing from the matrix to the interface to replace P and consequently the high Ge containing phase thio-LISICON II was formed. It should be mentioned that the Li_2S content in $Li_2S–P_2S_5$ of sample 3 is 50 mol%, which is much lower than 75 mol% as reported in Ref. [8]. In our studied system, we think some amount of P_2S_5 was not reacted with Li_2S, and as a glass network former, the rest P_2S_5 still kept in glass state in sample 3. This is why trace of Li_2S can be detected in the XRD diffraction patterns in Ref. [10] but ours are not.

The ionic conductivity of Sample 1, Sample 2 and Sample 3 as the function of reciprocal absolute temperature is shown in Fig. 3. Values of $\sigma_{30°C} = 2.9 \times 10^{-4}$ S cm^{-1} and $E_a = 0.39$ eV (the inset of Fig. 3) are observed for Sample 1 (without milling). After 4 h high-energy ball-milling (Sample 2), a phase transition from thio-LISICON III analog to thio-LISICON II analog was observed, and simultaneously, an increment of more than three times in ionic conductivity to 9.3×10^{-4} S cm^{-1} and a reduction in activation energy to 0.35 eV were achieved. The substantial improvement after the ball-milling is mainly ascribed to the formation of better-performance thio-LISICON II phase. The reduction of particle size caused by high-energy ball-milling should be the other reason. With further milling for 12 h (Sample 3), the thio-LISICON II phase kept unchanged and its particle size was further reduced. Solid electrolyte with smaller particle size is favorable of having higher density and good contact with electrode. An extremely high ionic conductivity of 1.5×10^{-3} S cm^{-1} was achieved, which is comparable to that of the most excellent LiSEs [8–12]. Furthermore, the hydrolyzation of the as-prepared sample should be effectively suppressed due to the nonhygroscopic property of the introduced $Ge_{0.35}Ga_{0.05}Se_{0.60}$ glass [16].

Fig. 4 shows the results of DC polarization measurement of Sample 3. When lithium plates were used as unblocking electrodes, an almost constant current of 1.3×10^{-2} A was observed, and the DC conductivity was calculated to be 1.6×10^{-3} S cm^{-1}. When using indium as blocking electrodes, the DC current initially

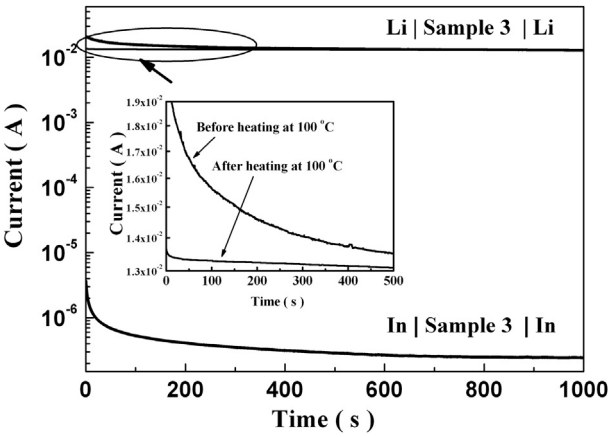

Fig. 4. Time dependence of currents for Sample 3 using blocking electrode and unblocking electrode, respectively. The insert shows the local magnification when using unblocking electrode.

decreased sharply due to the polarization [18,19] and then stabilized at 2.4×10^{-7} A after 400 s. The DC conductivity was calculated to be 2.3×10^{-8} S cm^{-1}, nearly four orders of magnitude lower than the value obtained by using lithium unblocking electrodes. Therefore, it can be concluded that the lithium ion transfer number is higher than 0.9999 and the electronic conduction at total conductivity in this selenide-containing electrolyte is almost negligible.

As locating below O and S in VIA group, selenides have higher valence band and narrower band gap than oxides and sulfides. Thus many researchers worry about that selenides might have narrow electrochemical window and low chemical stability against lithium metal. The electrochemical window and the chemical stability against lithium metal were not mentioned in all the former literature [13–15,20,21]. The experiment data show, however, the DC polarization curves are close to each other before and after heat treatment. They lie within the same order of magnitude and almost overlap after 800 s, indicating that almost no reaction occurred at the interface between the Sample and the lithium plates (Fig. 4). By zooming the initial parts of the two curves (inset of Fig. 4), it is found that the curve after heat treatment is more flat, implying the better cyclability of the sample. In view of the electrical conductivity of $Ge_{0.35}Ga_{0.05}Se_{0.60}$, it is in the color of brown, which means it has a wide band gap and its electrical conductivity should be very

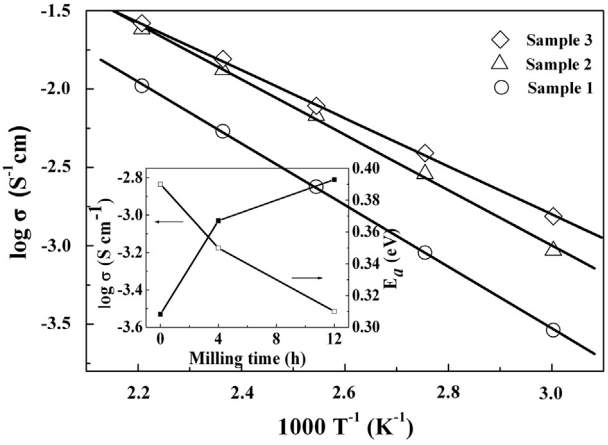

Fig. 3. Reciprocal temperature dependence of conductivities for Sample 1, Sample 2 and Sample 3. The inset depicts the $\sigma_{30°C}$ and E_a as the function of the milling time.

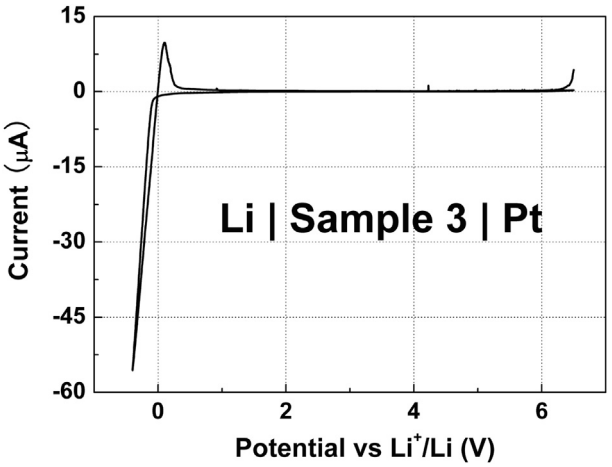

Fig. 5. Cyclic voltammetry for the asymmetry cell Li/Sample 3/Pt.

low. To verify this, DC polarization measurement was carried out on the amorphous $Ge_{0.35}Ga_{0.05}Se_{0.60}$ sample and its DC conductivity was calculated to be around 10^{-11} S cm^{-1}, which is also almost negligible.

As shown in Fig. 5, the electrochemical stability of Sample 3 was characterized by cyclic voltammogram. No significant current peaks were observed within the whole scan range, except for that due to cathodic and anodic lithium deposition/dissolution reactions near 0 V *vs.* Li^+/Li. So the as-prepared glass-ceramic sample was stable up to a wide electrochemical window 6.5 V, which is much higher than 4.5 V of the traditional liquid electrolyte.

4. Conclusions

A strategy was successfully designed to introduce nonhygroscopic $Ge_{0.35}Ga_{0.05}Q_{0.60}$ (Q = S, Se) into the Li_2S–xP_2S_5 system by partially substituting the hygroscopic P_2S_5 for the first time. The double substitution effect, partial substitution of Se at the S sites and Ge at the P sites, exists at the interface between $0.5Li_2S$-xP_2S_5 and $Ge_{0.35}Ga_{0.05}Se_{0.60}$ enhanced the lithium ion conductivity of the sample. The electrolyte of $0.5Li_2S$–$0.5P_2S_5$–$0.5Ge_{0.35}Ga_{0.05}Se_{0.60}$ has an extremely high ionic conductivity of 1.5×10^{-3} S cm^{-1} with negligible electronic conductivity and wide electrochemical window over 6.5 V. The excellent overall properties indicate that selenide-containing compounds can be promising candidates for high-performance LiSEs.

Acknowledgments

This work was financially supported by National Science Foundation of China (Grant Nos. 51125006, 91122034, 20901083, 21203234).

References

[1] C. Julien, G.A. Nazri, Solid State Batteries: Materials Design and Optimization, Kluwer Academic Publishers, 1994.
[2] T. Minami, M. Tatsumisago, M. Wakihara, C. Iwakura, S. Kohjiya, I. Tanaka, Solid State Ionics for Batteries, Springer-Verlag, Tokyo, 2005.
[3] Jos F.M. Oudenhoven, L. Baggetto, Peter H.L. Notten, Adv. Energy Mater. 1 (2011) 10–33.
[4] X.L. Ji, L.F. Nazar, J. Mater. Chem. 20 (2010) 9821–9826.
[5] N. Kamaya, K. Homma, Y. Yamakawa, M. Hirayama, R. Kanno, M. Yonemura, T. Kamiyama, Y. Kato, S. Hama, K. Kawamoto, A. Mitsui, Nat. Mater. 10 (2011) 682–686.
[6] R. Murugan, V. Thangadurai, W. Weppner, Angew. Chem. Int. Ed. 46 (2007) 7778–7781.
[7] V. Thangadurai, W. Weppner, Ionics 12 (2006) 81–92.
[8] R. Kanno, M. Murayama, J. Electrochem. Soc. 148 (2001) A742–A746.
[9] F. Mizuno, A. Hayashi, K. Tadanaga, M. Tatsumisago, Adv. Mater. 17 (2005) 918–921.
[10] A. Hayashi, S. Hama, T. Minami, M. Tatsumisago, Electrochem. Commun. 5 (2003) 111–114.
[11] J.E. Treveya, Y.S. Jungb, S.H. Lee, Electrochim. Acta 56 (2011) 4243–4247.
[12] T. Ohtomo, A. Hayashi, M. Tatsumisago, Y. Tsuchida, S. Hama, K. Kawamoto, J. Power Sources 233 (2013) 231–235.
[13] J.H. Kim, Y.S. Yoon, M.Y. Eom, D.W. Shin, Solid State Ionics 225 (2012) 626–630.
[14] T. Kaib, P. Bron, S. Haddadpour, L. Mayrhofer, L. Pastewka, T.T. Jarvi, M. Moseler, B. Roling, S. Dehnen, Chem. Mater. 25 (2013) 2961–2969.
[15] S.P. Ong, Y.F. Mo, W.D. Richards, L. Miara, H. Lee, G. Ceder, Energy Environ. Sci. 6 (2013) 148–156.
[16] M.A. Popescu, Non-Crystalline Chalcogenides, Kluwer Academic Publishers, London, 2000.
[17] T. Kaib, P. Bron, S. Haddadpour, M. Kapitein, P. Bron, C. Schroder, H. Eckert, B. Roling, S. Dehnen, Chem. Mater. 24 (2012) 2211–2219.
[18] H. Morimoto, H. Yamashita, M. Tatsumisago, T. Minami, J. Am. Ceram. Soc. 82 (1999) 1352–1354.
[19] S. Kohjiya, T. Kitade, Y. Ikeda, A. Hayashi, A. Matsuda, M. Tatsumisago, T. Minami, Solid State Ionics 154–155 (2002) 1–6.
[20] S.T. Kong, O. Gun, B. Koch, H.J. Deiseroth, H. Eckert, C. Reiner, Chem. Eur. J. 16 (2010) 5138–5147.
[21] V. Epp, O. Gun, H.J. Deiseroth, M. Wilkening, Phys. Chem. Chem. Phys. 15 (2013) 7123–7132.